

The Formation of a Cooling Layer in a Partially Optically Thick Shock

A. B. Reighard · R. P. Drake

Received: 13 April 2006 / Accepted: 21 August 2006
© Springer Science + Business Media B.V. 2006

Abstract The mechanics of a radiative shock which has “collapsed,” or been compressed to high density, via radiative cooling is discussed. This process is relevant to an experiment in xenon gas that produced a driven, radiatively collapsed shock, and also to a simulation of the supernova 1987A shock wave passing through the outer layers of the star and into the low-density circumstellar material.

Keywords Radiation · Radiation hydrodynamics · Optically thick shock · Driven shock · Collapsed shock · Laboratory astrophysics

Introduction

To reach a regime where the transport of radiation through a system can affect the hydrodynamic properties of the material, two conditions must be met. Firstly, one must create a system with sufficient “optical depth,” a measure of the attenuation of radiation. Said another way, there must be enough material that the radiation is affected by its presence. This system must also be relatively hot, on the order of at least tens of eV. This can be difficult in laboratory systems, requiring energy sources capable of delivering high laser power or X-ray flux to a small target, driving shock waves into materials of relatively low density. In astrophysics, energetic explosions into diffuse material, like a supernova explosion, produce similar effects.

We have performed experiments at the Omega laser that have created a planar, driven, radiatively collapsed shock wave in xenon gas. This system is optically thick (highly absorptive of radiation) downstream in the shocked gas, and

after a brief transition period where the upstream gas is ionized by precursor radiation, optically thin upstream in the unshocked gas. This experiment (described further in Reighard et al. (2006)) has produced a shock wave that radiated away enough energy to cool both the electrons and the ions in the shocked material, causing the gas to become highly compressed in response. A metrology image of a target used in this experiment is shown in Fig. 1a. The beryllium drive surface is in the lower right-hand corner of the image, mounted on a polyimide tube 5 mm in length and 0.6 mm OD. Shown in Fig. 1b is a radiograph of collapsed xenon gas in this experiment, taken via side-on backlit pinhole radiography. The shock is moving to the right in this figure, where the x coordinate is the distance along the target axis from the initial position of the drive disk, while the y coordinate is the radial coordinate of the target. The dense xenon shows as a dark absorption feature. The shock front is just to the right of the dark absorption feature. The shape of the dense collapsed layer is affected by line of sight of the diagnostic and drag along the walls of the target, as well as any non-uniformity in the production of the layer from instabilities.

It is then natural to seek astrophysical shocks with the same optical depth structure for comparison to this system. In an article by Ensman and Burrows, (1992), 1D hydrodynamic simulations of shock breakout in SN 1987A show a highly compressed, cooled shock as the disturbance passes through the outer layers of the star and into the lower density circumstellar material. The temperature and density profiles show a remarkable similarity to temperature and density profiles calculated in the experiment described above, as shown in Fig. 2. The density and temperature profiles for the experimental system in Fig. 2b. were generated using Hyades (Larsen and Lane, 1994), a 1D lagrangian code with a three-fluid treatment of the material and a multigroup treatment of the radiation with flux-limited diffusion.

A. B. Reighard (✉) · R. P. Drake
Department of Atmospheric, Oceanic, and Space Sciences,
University of Michigan, Ann Arbor, MI 48109, USA

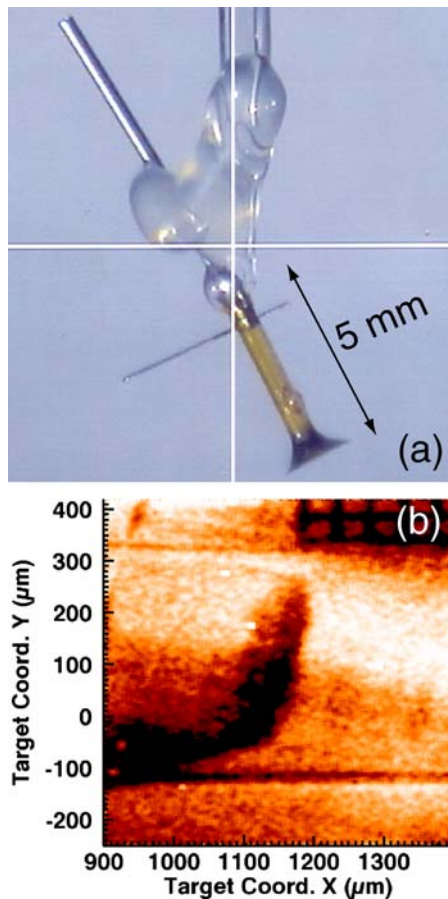


Fig. 1 (a) Metrology image from experiments described in Reighard et al. Drive beams hit a Be disk (lower right corner of image), and accelerate it into the xenon filled plastic tube. The experiment is approximately 5 mm long. (b) Data image from Reighard et al. at 8.2 ns after drive beams turn on. The thin layer of collapsed xenon shown by X-ray radiography is approximately $65 \mu\text{m}$ thick, and has an average velocity of 140 km/sec. The gold grid used as a spatial and magnification indicator is in the top right of the image, while the edges of the target tube are visible as horizontal lines near the bottom and top of the image

These systems will produce this kind of collapsed shock structure in fundamentally the same way. This begs a causal explanation of the physics producing this structure in both systems. Here, we offer a step-by-step explanation of the physics behind the formation of a collapsed radiative shock. For each step in the discussion, parameters from the experiment described above (and in more complete detail in Reighard et al. (2006)) are used as an example.

Radiatively collapsed shock formation

As in any shocked system, a shock wave heats ions as it passes through cold material. The shock accelerates everything to a higher velocity, but most of the energy of the shock goes into heating the heavier ions. This happens quickly, over the span

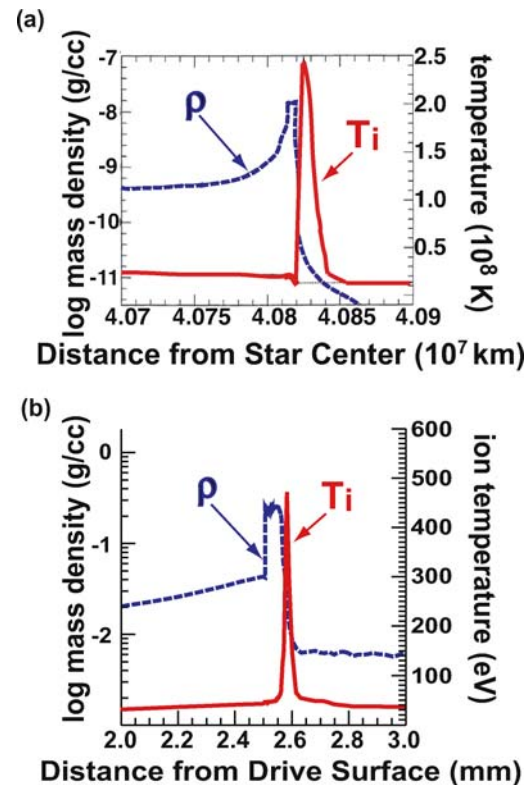


Fig. 2 1D Lagrangian simulations of the two systems discussed. (a) 1D VISPHOT calculation adapted from Ensmann and Burrows (1992). (b) 1D Hyades simulation of discussed experimental system. Both systems show a layer of highly compressed material accompanied by quick cooling through a region that is thin compared to the distance the shock has traveled

of just a few ion-ion mean free paths. Through conservation equations, the matter is also compressed by a certain amount, depending on the polytropic index of the material, and the pressure increases.

In an ionized system that can exchange energy by collisions, the ions begin to transfer energy to the cooler electrons. The rate at which this happens is dictated by the ion-electron collision rate, ν_{ie} , given by

$$\nu_{ie} = 3.2 \times 10^{-9} \frac{n_i Z^3 \ln \Lambda}{A T_e^{1.5}}, \quad (1)$$

where n_i is number density in cm^{-3} , Z is the average ionization state, $\ln \Lambda$ is the coulomb logarithm, A is the atomic weight of the material, and T_e is electron temperature in eV (Drake, 2006). The rate of ion cooling depends on the difference between the ion temperature and the electron temperature;

$$\frac{\partial T_{\text{ion}}}{\partial t} = -\nu_{ie}(T_{\text{ion}} - T_e). \quad (2)$$

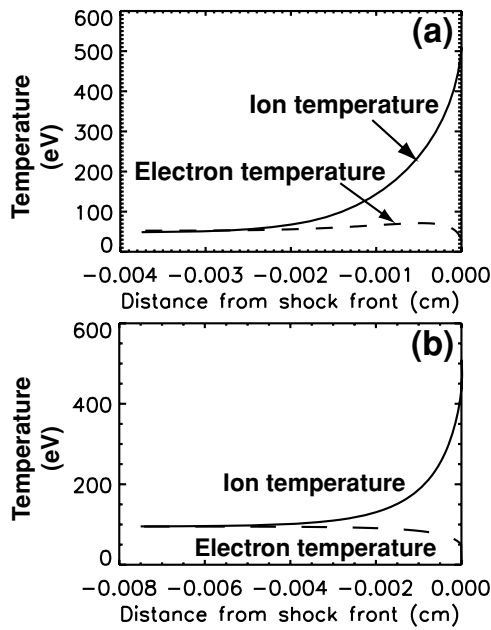


Fig. 3 Ion and electron temperatures behind the shock front for the parameters from the experimental system, assuming a shock moving at 150 km/sec. The shock front is located at 0 cm. (a) Temperature profiles with only collisional heat exchange. (b) Temperature profiles with both collisional heat exchange and radiative cooling of the electrons. In this system, radiative cooling becomes important before collisional heat exchange can equilibrate the electron and ion temperatures

This process slows as the temperatures equilibrate. In xenon gas, with $n_i = 1.5 \times 10^{19}$, $A = 131.3$, with initially T_e negligible, and T_i approximately 500 eV, this equilibration process takes on the order of a few hundred picoseconds. The ion and electron temperature profiles from collisional heat exchange in xenon gas are shown in Fig. 3a. The initial ion temperature is dictated by the strong shock equations for a shock wave moving at 150 km/sec, for which the equilibration length would be approximately 30 μm . This calculation is relevant to the experimental system described above, where a driven shock moves through xenon gas at velocities in excess of 100 km/sec. 1D Hyades simulations give a similar result, showing a equilibration length of approximately 25 μm at an instantaneous velocity of 160 km/sec.

In some systems, the electron temperature may become large enough to cause the free electrons in the system to radiate. As the electrons in the system get warmer, they begin to radiate more. Though electrons in the system may continue to gain energy from collisions with ions, now they may also cool through radiative losses, at a fractional energy radiation rate given by the ratio of the radiative flux from two surfaces of a planar slab, $2F_{\text{rad}}$ to the energy content of the shocked material of density ρ , slab thickness d , specific opacity κ , and specific heat (per unit T_e) c_v . This ratio is

$$\nu_{\text{rad}} = \frac{2F_{\text{rad}}}{\rho d c_v T} = \frac{2\kappa d \rho \sigma T_e^4}{\rho d c_v T} \tag{3}$$

for an optically thin material, where σ is the Stefan-Boltzmann constant. On the approximation that $T = ZT_e + T_i = (Z + 1)T_e$ if $T_e \approx T_i$, where Z is the average ionization state, this rate simplifies to

$$\nu_{\text{rad}}^* = 2.2 \frac{A}{(Z + 1)} \kappa T_e^3 \tag{4}$$

in sec^{-1} for T_e in eV and κ in cm^2/g . For the model calculation presented, we evaluated κ to be 2500 cm^2/g using a SEASAME table value for xenon at 100 eV, averaged over values for relevant densities (Leibrandt et al., 2005). If the collisional heating happens quickly, the heating and cooling of electrons may be treated as a two-step process. For the experimental system, significant radiative cooling begins before the ion and electron temperatures equilibrate, so the two-step approximation does not hold. Figure 3b. shows the temperature profiles produced by the combination of electron-ion heat exchange and radiative losses evaluated as just described.

If the shocked gas can quickly radiate away a significant fraction of its energy, the system will form a collapsed layer in response to this loss. The cooling layer, where radiation cools the system, must be optically thin for energy to escape. As the electron temperature rises in the system not only will the radiative rate become large, the opacity of the system κ will decrease, making the hot material optically thin, allowing the energy to escape via radiation.

As the shocked material loses energy, the system must respond to keep certain parameters constant across the shock. The conservation equations for mass and momentum must still hold, given by

$$\rho_1 u_1 = \rho_2 u_2 \tag{5a}$$

$$p_1(\rho, T) + \rho_1 u_1 = p_2(\rho, T) + \rho_2 u_2. \tag{5b}$$

Pressure, density, and temperature are linked through these equations, so as the temperature drops another quantity must respond to keep the system in balance. If the pressure were to drop, there would be a void in the system, and the material would compress in response to energy loss. Pressure can be expressed as a function of temperature and density using the ideal gas law,

$$p = \rho R T_i, \tag{6a}$$

where R is the gas constant,

$$R = \frac{(Z + 1)k_B}{Am_p}, \tag{6b}$$

and k_B is Boltzmann's constant.

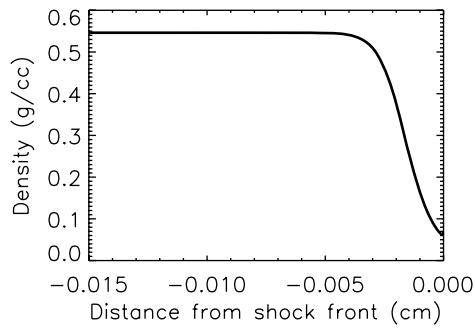


Fig. 4 Density profile when affected by radiation losses. In this simple analytic model, the radiative transfer equation was not fully employed, nor was the influence of increasing opacity as electron temperature decreased. Both these factors would affect the final density of the cooling layer. Here, the final density is dictated by the loss of all electron energy via radiation

Estimating the density profile from this kind of relationship requires some understanding of how the “gas constant” R changes with ionization. Using an estimate of how the average ionization Z changes with temperature allows an estimate of R . Using the Saha equation to calculate the average ionization state (only strictly valid in a equilibrium distribution, where ionization balances recombination exactly), Z_{bal} is

$$Z_{\text{bal}} = 19.7 \sqrt{T_e(1 + 0.19) \ln \left(\frac{T_e^{3/2}}{n_{24}} \right) - \frac{1}{2}}, \quad (7)$$

where T_e is in eV and n_{24} is number density in units of 10^{24} cm^{-3} . Given these substitutions, pressure can be expressed solely as a function of temperature and density. The density profile can then be calculated from the temperature profile and the momentum conservation equation. While the profile generated in this way should be qualitatively correct, one would need to solve the radiative transfer equation to actually predict the final density value, taking into account the amount of radiation emitted and absorbed in each differential slab. In Fig. 4 we show the qualitative profile of radiative collapse, here without a full treatment of the radiative transfer. The layer continues to collapse until the system has radiated away all of the thermal energy of the system, where the electron temperature approaches zero, and the ion temperature is very low. Therefore in this incomplete model, the final value of the compression is not indicative of the value produced in the experimental systems.

As the system becomes more compressed, the optical depth of the dense, collapsed layer increases, and the opacity can change as the system cools. As the optical depth of the material increases, it becomes more difficult to remove energy from within the dense material, in response to which the rate of density increase eventually reaches zero. If the system relaxes to a quasi-steady state, where the shocked

system maintains the same general shape, the ultimate thickness of the layer will depend on the balance of energy flowing through the layer. The optically thick downstream material will radiate at its blackbody temperature. This radiation will pass through the optically thin cooling layer but must be balanced by the radiation from the cooling layer to have steady state. The cooling layer will radiate equally both upstream and downstream. Because it is optically thin, the upstream, unshocked gas will radiate negligibly, and energy will escape from the system through it. Flux at the boundaries of the layer coupled with the hydrodynamic equations then give the final, post-shock temperature and the spatial extent of the cooling layer, as discussed in more detail in Drake (2006).

In a driven system like the experiment described, the amount of momentum in the system is fixed. As the piston driving the shock amasses collapsed xenon, the system will decelerate. It is possible that the system will eventually slow to the point where the driving forces no longer heat the system to the point where radiation cooling can be effective. At this point, the evolution of the shock will become hydrodynamic in nature, and radiative collapse will cease.

Conclusion

Radiative cooling in a system that is optically thick downstream (behind the shock) and optically thin upstream (in the unshocked material) can lead to dramatic effects in the overall structure of the shocked material. Collapse via radiative cooling of the shocked gas can lead to compression of material to much higher densities than those in a strong shock with no radiative cooling.

Future work includes analysis of radiative effects at different initial driving velocities. This is achieved by varying the thickness of the Be layer illuminated by the laser. Computational efforts include work to better understand the effects of opacity on xenon at temperatures between 50 and 200 eV. In addition, by watching the long-term evolution of the shocked layer, such experiments might observe the onset of hydrodynamic instabilities like those discussed by Vishniac and Ryu (1989). Beyond such work, this type of system could be developed as a radiation source for experiments to examine other issues such as radiation transport.

Acknowledgements The authors acknowledge the vital contributions of the Omega technical staff and the target fabrication group at the University of Michigan. This work is supported by the National Nuclear Security Agency under DOE grants DE-FG03-99DP00284 and DE-FG03-00SF22021, and by other grants and contracts.

References

- Drake, R.P.: High Energy Density Physics: Foundations of Inertial Fusion and Experimental Astrophysics. (Springer, New York, 2006)
- Ensmann, L., Burrows, A.: *ApJ* **393**, 742 (1992)
- Larsen, J.T., Lane, S.M.: *J. Quant. Spectrosc. Radiat. Transfer* **51**(1), 179 (1994)
- Leibrandt, D.R., Drake, R.P., Reighard, A.B., et al.: *ApJ* **626**, 616 (2005)
- Reighard, A.B., Drake, R.P., Dannenberg, K.K., et al.: *Phys. Plasmas* **13**, 082901 (2006)
- Vishniac, E.T., Ryu, D.: *ApJ* **337**, 917 (1989)